October 1989

# PERFORMANCE MEASUREMENTS IN 3D IDEAL MAGNETOHYDRODYNAMIC STABILITY COMPUTATIONS

David V. Anderson, W. Anthony Cooper,
Ralf Gruber, Ulrich Schwenn

# PERFORMANCE MEASUREMENTS IN 3D IDEAL MAGNETOHYDRODYNAMIC STABILITY COMPUTATIONS

David V. Anderson[1], W. Anthony Cooper, Ralf Gruber[2],

Ulrich Schwenn[3]

Centre de Recherches en Physique des Plasmas

Association Euratom - Confédération Suisse

Ecole Polytechnique Fédérale de Lausanne

21, Av. des Bains, CH-1007 Lausanne, Switzerland

## Abstract :

The 3D ideal magnetohydrodynamic stability code TERPSICHORE has been designed to take advantage of vector and microtasking capabilities of the latest generation CRAY computers. To keep the number of operations small most efficient algorithms have was been applied in each computational step. The program investigates the stability properties of fusion reactor relevant plasma configurations confined by magnetic fields. For a typical 3D HELIAS configuration that has been considered we obtain an overall performance in excess of 1 Gflops on an eight processor CRAY-YMP machine.

[1]    NMFECC, Livermore, USA

[2]    GASOV, EPFL, Lausanne, Switzerland

[3]    MP-IPP, Garching, F.R.G.

# 1. Introduction

The advent of powerful vector and multiprocessor supercomputers with large memories like the Cray-YMP and the Cray-2 has made the investigation of the magnetohydrodynamic (MHD) stability properties of fully three-dimensional (3D) plasma configurations confined with magnetic fields feasible. The computer code TERPSICHORE has been developped for this purpose and has been explicitly designed to take advantage of the vector and microtasking capabilities of these types of computers.

To successfully tackle the linear stability problem in three dimensions using numerical methods, the computer program that is devised must be very carefully designed because compared with the 2D predecessors such as ERATO [1] or PEST [2] the memory and the CPU requirements can be correspondingly much larger. To become a useful tool, the 3D stability code must also be very fast in order to have the capability of exploring the larger parameter space associated with the extra degree of freedom that the third dimension introduces. In the construction of TERPSICHORE we have greatly benefitted from the accumulated experience developed in the design and operation of the 2D stability packages ERATO, PEST, PEST2 [3] and the code of Degtyarev et al. [4]. Thus, double Fourier expansions in the poloidal and toroidal angles and a finite hybrid element approach [5] are performed to optimally describe the eigensolution. In order not to include unnecessary modes a special expert-system-like program is used to select those poloidal and toroidal Fourier terms which contribute to the instability. This leads to minimum size matrices in the generalized eigenvalue problem. As a consequence, it is no longer the eigenvalue solver but rather the construction of the matrix elements that becomes the most expensive computational step. Special care has been taken to compute the double Fourier flux tube integrals of equilibrium quantities to construct each matrix element in most optimal way. These features clearly distinguish this code from its 2D predecessors which were developed in the mid seventies and were partially designed to benefit only from the vector and memory capabilities of Cray-1 computers that were available at that time. As a result, the TERPSICHORE code, although intended to be used as a 3D MHD stability package, performs the 2D stability problem much more efficiently and rapidly than either ERATO or PEST. In more complicated 3D low magnetic shear stellarator configurations we achieve an overall performance of over one Gigaflop/s on an eight processor Cray-YMP machine. The parallelization needed to achieve this high rate was entirely done by autotasking.

# 2. The physics problem

The 2D stability packages have been employed extensively in the last 10-15 years in the design of axisymmetric Tokamak devices such as the Joint European Torus (JET) and the Tokamak Fusion Test Reaction (TFTR) that have already been built and have operated successfully. They are presently being used to design reactor-like devices such as the International Test Experimental Reactor (ITER) which is an international collaborative effort to consider the next step in magnetic fusion energy research. The purpose of the ideal MHD stability codes is to determine the possible boundaries of operation in the plasma current and in the pressure that can be confined. As a testament to the sucess of these codes was the extraction of the Troyon limit [6] from computer simulations which was subsequently verified experimentally. It should be noted that a substantial fraction of the computational effort in magnetic fusion energy research realized on Cray computers in the last 10 years has been devoted to the 2D stability problem.

There are strong motivating factors to extend the stability analysis to 3D configurations. First, the experimental conditions in tokamaks display in many cases highly nonsymmetric internal magnetic structures. Second, external helical windings are incorporated in many tokamak designs for disruption control (which is a class of instability described by resistive MHD in the nonlinear phase rather than by the linear ideal MHD model) that can significantly alter the symmetry properties of the device. In the near term, a modification of the JET machine is planned to experimentally test this concept. Third, though present devices like JET have 32 toroidal magnetic field coils to minimize the magnetic ripple effects and force the configurations to be as close to axisymmetric as possible, the accessibility to the plasma and cost considerations constrain future larger tokamak designs to be built with a reduced number of toroidal coils that will as a result spoil the symmetry and increase the relevance of 3D calculations. Finally, a fourth important motivating factor, is the recent interest in - and relative success of stellarator configurations that employ external coils rather than transformer-induced plasma currents to generate the confining magnetic fields, and thus offer the attractive potential of steady state operation. These types of devices, of course, are inherently 3D in character.

To explore the problem of the linear MHD stability of confined plasmas, a variational form is constructed from the MHD equations combined with Maxwell's equations that can be expressed as [5]

$$\delta W_p + \delta W_v - \omega^2 \, \delta W_k = 0 \tag{1}$$

where $\delta W_p$ represents the potential energy in the plasma, $\delta W_v$ represents the magnetic energy in the vacuum region that surrounds the plasma, $\delta W_k$ represents the kinetic energy and $\omega^2$ corresponds to the eigenvalue of the system.

In 2D, it is straight forward to rigourously demonstrate that the MHD equilibrium consists of nested magnetic flux surfaces. A similar proof does not exist in 3D. Consequently, as a first

step, we have imposed the condition of flux surface nestedness in the underlying 3D equilibrium state we wish to investigate. We thus exclude cases with magnetic islands and internal separatrices. The potential energy can then be described as

$$\delta W_p = \frac{1}{2} \int \int \int d^3x \left[ C^2 + \gamma p |\nabla \cdot \vec{\xi}|^2 - D|\vec{\xi} \cdot \nabla s|^2 \right] \qquad (2)$$

where $\xi$ represents the perturbed displacement vector,

$$C = \nabla \times (\vec{\xi} \times B) + \frac{j \times \nabla s}{|\nabla s|^2}(\vec{\xi} \cdot \nabla s), \qquad (3)$$

$$D = \frac{2(j \times \nabla s) \cdot (B \cdot \nabla)\nabla s}{|\nabla s|^4}. \qquad (4)$$

B is the equilibrium magnetic field, $j = \nabla \times B$ is the equilibrium current density, p is the equilibrium pressure and $\gamma$ is the adiabatic index. The radial variable s labels the magnetic flux surfaces within the plasma domain $0 \leq s \leq 1$ from the magnetic axis to the plasma-vacuum interface. The vacuum energy is described as

$$\delta W_v = \frac{1}{2} \int \int \int d^3x \, (\nabla \times A)^2 \qquad (5)$$

where A is the perturbed vector potential. There are two methods to treat this part of the problem. One is to employ a Green's function technique and the other is to consider the vacuum as a pseudoplasma and in such case the structure of the resulting matrix equation is virtually identical to that inside the plasma. The applications discussed in this paper are limited to internal plasma instabilities to which $\delta W_v$ does not contribute, thus further details about the vacuum treatment are omitted.

A convenient form to represent the perturbed displacement vector is

$$\vec{\xi} = \sqrt{g}\xi^s \nabla\theta \times \nabla\phi + \eta\frac{(B \times \nabla s)}{B^2} + \left[ \frac{J(s)}{\Phi'(s)B^2}\eta - \mu \right] B \qquad (6)$$

where $\theta$ and $\phi$ are the poloidal and toroidal angles, respectively, of the Boozer magnetic flux coordinate system which we have chosen for the stability analysis. This particular choice of coordinate system is optimal for the stability calculations because in its representation two very important conditions are satisfied. First, that the magnetic field lines are straight which allows a compact and efficient determination of the $B \cdot \nabla$ operator and thus an accurate description of the resonant surfaces. Second, it allows the most precise description of the parallel current (which is an important driving mechanism of instabilities in 3D systems) because the poloidal and toroidal magnetic fields in the covariant representation are current fluxes. The radial,

4

binormal and parallel components of the perturbation vector are given by $\xi^s$, $\eta$ and $\mu$, respectively. The Jacobian of the transformation from cylindrical to Boozer coordinates is denoted by $\sqrt{g}$, $J(s)$ is the toroidal current flux function, $\Phi(s)$ is the toroidal magnetic flux function and prime(') indicates the derivative of a flux surface quantity with respect to the radial variable s.

Noting that the perturbation component $\mu$ appears only in the term $\nabla \cdot \xi$ of $\delta W_p$, we impose the incompressibility constraint to eliminate it algebraically from the problem. This, however, implies that correct instability growth rates can no longer be computed, but the points of marginal stability are unaffected. Although we abandon the determination of growth rates, this procedure offers the advantage of reducing the size of the stability problem because only two instead of three components of the perturbation have to be calculated. This leads in addition to a reduction of coupling effects and the advantage of increased accuracy in the determination of marginal stability points because the continuous spectrum becomes displaced. This allows the application of interpolation rather than extrapolation techniques in the calculation. This approach was previously adopted in the development of the PEST2 code [3] which considerably speeded up and improved the accuracy of marginal stability computations compared with the 2D PEST stability package [2].

We apply a Fourier series decompostion of the perturbation components $\xi^s$ and $\eta$ given by

$$\xi^s(s,\theta,\phi) = \sum_{l} s^{-q_l} X_l(s)\sin(m_l\theta - n_l\phi + \Delta) \tag{7}$$

and

$$\eta(s,\theta,\phi) = \sum_{l} Y_l(s)\cos(m_l\theta - n_l\phi + \Delta) \tag{8}$$

where $l$ is an index that labels the mode number pair $(m_l, n_l)$, $\Delta$ is a phase factor, and the exponent $q_l = 0$ for $m_l \neq 1$ or $q_l = 1$ for $m_l = 1$. Then to satisfy regularity conditions at the origin, we have $X_l(0) = 0$. We employ a finite hybrid element radial discretisation because radial derivatives act only on $X_l$. As result, the energy principle described in Eq. (1) reduces in the weak form to an eigenvalue problem of the form

$$Ax = \lambda Bx \tag{9}$$

where $x = (X_l, Y_l)$, the eigenvalue is $\lambda = \omega^2$, the matrix A is symmetric and block diagonal. As a result of imposing the incompressibility constraint, it is convenient to choose the matrix B that represents $\delta W_k$ to be the unit matrix. The Fourier decomposition of the perturbation components $\xi^s$ and $\eta$ leads to the appearance in the matrix elements of A of what we referred to in the introduction as double Fourier flux tube integrals. Extensive algebraic manipulations were performed to reduce the number of these integrals to a total of seven as they can represent a

significant fraction of the computational effort for realistic configurations. Typically, they are of the form

$$C_{lk}^{(2)}(s) = 2L_s/4\pi^2 \int \int d\theta \, d\phi \, \sqrt{g} \, \sin(m_l\theta - n_l\phi + \Delta) \, \sin(m_k\theta - n_k\phi + \Delta)$$

$$C_{lk}^{(3)}(s) = 2L_s/4\pi^2 \int \int d\theta \, d\phi \, (g_{ss}/\sqrt{g}) \, \sin(m_l\theta - n_l\phi + \Delta) \, \sin(m_k\theta - n_k\phi + \Delta) \qquad (10)$$

$$C_{lk}^{(4)}(s) = 2L_s/4\pi^2 \int \int d\theta \, d\phi \, (g_{s\theta}/\sqrt{g}) \, \sin(m_l\theta - n_l\phi + \Delta) \, \sin(m_k\theta - n_k\phi + \Delta)$$

where the limits of integration are given by $0 \leq \theta \leq 2\pi$ and $0 \leq \phi \leq 2\pi/L_s$ and $L_s$ corresponds to the number of periods of the instability structure in one toroidal transit. For most cases of interest, $L_s = 1$. The quantities $g_{ss}$ and $g_{s\theta}$ are lower metric elements.

# 3. The organization of TERPSICHORE

The stability code TERPSICHORE consists of 6 basic modules, categorised as

(a) Interface to the MHD equilibrium

(b) Reconstruction of the MHD equilibrium

(c) Mapping the MHD equilibrium

(d) Construction of the stability matrix elements

(e) Eigenvalue solver

(f) Analysis and diagnostics of the results

The philosophy that underlies the construction of the routine that interfaces TERPSICHORE with an MHD equilibrium code is to rely on the minimum amount of information that is necessary and then subsequently reconstruct the equilibrium. This information consists basically of the geometry as well as the poloidal and toroidal magnetic fluxes. Thus, from the 3D MHD equilibrium code VMEC [9], which we have used exclusively so far as the source of 3D equilibria with nested flux surfaces, we obtain the Fourier amplitudes of the inverse coordinates R (the distance from the major axis) and Z (the distance from the midplane) to specify the geometry of the configuration. We also obtain from it $\Phi'(s)$ and $\psi'(s)$ which are the radial derivatives of the toroidal and poloidal magnetic flux functions, respectively. The computational effort in the interface is negligible. The reconstruction of the MHD equilibrium, on the other hand, constitutes a large fraction of the computer time that is spent. The Jacobian and metric elements in the original coordinates of the MHD equilibrium code are developed. The periodic poloidal angle renormalisation function [9] is computed in each flux tube by solving a linear elliptic partial differential equation that results from the condition $\mathbf{j} \cdot \nabla s = 0$ using Fourier techniques. The current densities are calculated and the accuracy of the reconstructed equilibrium is tested. The coordinate system that is optimal for the computation of 3D MHD equilibria using inverse Fourier methods consists of that in which the spectrum of modes required to obtain the equilibrium to a specified accuracy is minimized. It does not, in general, coincide with the Boozer coordinate system which, as we have discussed earlier, is optimal for the stability analysis of 3D systems. Thus, we have to perform a mapping from the coordinates of the equilibrium to the Boozer coordinates. From the expansion of the magnetic field in the covariant representation in the equilibrium coordinates, we obtain an auxiliary function that is

required for the mapping procedure [10]. We then calculate the Fourier amplitudes of Boozer coordinate quantities (i.e. R, Z, $B^2$, etc.) directly from information in the real space equilibrium grid. Further details about the mapping procedure we have implemented can be found in Ref. 7. We then calculate the Jacobian and the metric elements that correspond to Boozer coordinates in real space, we test the accuracy of the equilibrium we have constructed in Boozer coordinates and develop additional quantities that are required for the stability analysis. This part usually constitutes a moderate fraction of the computational requisites.

We proceed next to the fourth step, which is the computation of the elements of the matrices A and B. We first read in a table of instability modes that are selected for the calculation. As mentioned earlier, the matrix B is unity and therefore trivial to construct. We separate out the seven double Fourier flux tube integrals that appear in the elements of A to design a routine that is highly vectorizable and parallelizable as this can represent a dominant fraction of the overall computational time if this part is not carefully treated. The eigenvalue solver inverts the matrix A to determine the eigenvalue and the eigenvectors using an inverse vector iteration method. This solver has been very carefully designed so that it uses only a very small portion of the computer time. Finally, in the analysis and diagnostic sections, the kinetic and potential energies are reconstructed, the eigenvalue is tested, the parallel component of the displacement vector is calculated and the components of the perturbation in real space are determined. The computational effort here is negligible.

# 4. The test case

As a test case to investigate the performance and capabilities of the TERPSICHORE code, we have chosen a 4 field period Helias stellarator configuration [11] that has been considered as a candidate for the Wendelstein VII-X device that is being planned as the next step in stellarator experiments at the Max Planck Institut für Plasma Physik in the Federal Republic of Germany. As can be seen in the first two figures, the configuration we shall examine represents a particularly nontrivial test for the TERPSICHORE code. Its stability properties are not amenable to treatment by the stellarator expansion method because it has a helical magnetic axis, thus a fully 3D approach must be followed.

The coils that generate the toroidal and poloidal confining magnetic fields in one period of the device are shown in Fig. 1. One can also perceive the shape of the plasma as it twists within the coil structure. The cross sectional cut at one end of the field period shown reveals the shape of the internal flux surfaces. To obtain these, several magnetic field lines at different radial locations were followed around the torus for a very large number of transits. Each point that appears in the figure corresponds to the intersection of one of the field lines with the vertical plane. Each field line that is followed thus yields a series of points on the plane that traces out a flux surface. The three dimensional character of a flux surface over the entire 4 period toroidal domain can be more clearly appreciated in Fig. 2.

The 3D MHD Helias equilibrium we investigate was generated with the VMEC code [9]. The volume averaged beta, which is a measure of the ratio between the plasma pressure and the confining magnetic field energy density was $\beta = 2\%$ for this case with vanishing net toroidal plasma current within each flux surface. The number of radial intervals was $N = 48$ and the number of modes needed to describe the equilibrium state was $N_e = 50$. In addition to the mode selection table, we obtain from VMEC the Fourier amplitudes R and Z, as well as $\Phi'(s)$ and $\psi'(s)$ on each flux surface. The number of modes required to reconstruct the equilibrium state in the Boozer coordinates was $N_b = 160$. Note that the Boozer spectrum is much broader than that of the original equilibrium coordinates. This demonstrates that the direct computation of the MHD equilibrium in the Boozer coordinates would be inefficient and possibly unfeasible. To prepare the computation of the Fourier integrals, the number of intervals in the poloidal angle variable and in the toroidal angle variable were chosen as $N_p = 72$ and $N_t = 32$, respectively.

The selection table of modes to describe the internal plasma instability structures for this device was chosen to have $N_s = 32$ modes. The stability analysis computed with TERPSICHORE demonstrated that this configuration was weakly unstable. The magnitude of the most unstable eigenvalue was $\lambda = -1.67 \times 10^{-3}$. The corresponding eigenmode structure on the toroidal plane that has $\phi = 0$ is shown in Fig. 3. The dominant structure corresponds to an m = 4, n = 3 mode localized about the surface with rotational transform $\iota(s) \equiv d\psi/d\Phi = 0.75$. It should be noted that coupling effects to sidebands represent an important aspect in driving this instability.

# 5. Performance measurements

## 5.1. Operation counts

The operation counts for all important time consuming computational steps mentioned in chapter 3 give:

(b) *Reconstruction of the MHD equilibrium:*

$$O_r = 34 \, N \, N_p \, N_t \, N_e + N \, N_p \, N_t \, N_b \, (6.5 \, N_b + 75) + 2 \, N \, N_b^3$$

(c) *Mapping of the MHD equilibrium:*

$$O_m = 144 \, N \, N_p \, N_t \, N_b$$

(d) *Construction of the stability matrix elements:*

$$O_f = 14.5 \, N \, N_p \, N_t \, P \, N_s^2$$

(e) *Eigenvalue solver :*

$$O_e = 20 \, N \, N_s^3 + 38 \, N \, N_s^2 \, N_{it} \, ,$$

where

| | |
|---|---|
| $N$ | Number of radial flux tubes |
| $N_p$ | Number of poloidal points for the Fourier integrals |
| $N_t$ | Number of toroidal points for the Fourier integrals |
| $N_e$ | Number of Fourier terms in equilibrium |
| $N_s$ | Number of Fourier terms in stability |
| $N_b$ | Number of Fourier terms to represent equilibrium and geometrical quantities in Boozer coordinates |

P      Number of equilibrium periods

$N_{it}$    Number of inverse iteration steps in the eigenvalue solver

For the practical Helias case ( $N=48$, $N_p=72$, $N_t=32$, $N_e=50$, $N_s=32$, $N_b=160$, $P=4$, $N_{it}=11$), the following operation counts are obtained:

$$O_r = 20.0 \times 10^9$$
$$O_m = 2.6 \times 10^9$$
$$O_f = 6.8 \times 10^9$$
$$O_e = 0.1 \times 10^9$$

leading to a total of $29.5 \times 10^9$ operations. The reconstruction of the equilibrium solution which includes the preparation for the most efficient evaluation of the Fourier integrals takes 68% of them, the mapping 9%,and the Fourier integrals 23%. The timing of the eigenvalue solver is negligible.

## 5.2. Parallelization procedure

Before attempting procedures that effect the parallelization of the TERPSICHORE code, the double Fourier flux tube integrals that appear in the subroutines in which the MHD equilibrium is reconstructed and in the subroutines in which the elements of the stability matrix A are determined are treated with successive applications of the Cray Research, Inc. mathematical routine MXM that performs matrix multiplications. Although this entails an increase in the number of floating point operations and in the storage requirements, the very efficient vectorization properties of the MXM routine reduces the computational time substantially. The bulk of the computational effort is concentrated in three subroutines. These calculate the periodic poloidal angle renormalization function, the mapping of the MHD equilibrium to Boozer coordinates and the elements of the stability matrix A. The time consumption in these subroutines is caused by repeated calls to MXM and to routines that evaluate trigonometric functions. We tried at first to parallelize only these three particular routines, and although notable improvements in performance were achieved, we deemed these to be unsatisfactory.

The optimal performance realized with the TERPSICHORE code was obtained with the application of Cray Research autotasking utilities through the activation of options available on the *cf77 -Zp* compiler to all the subroutines in the program with the exception of the interface to the MHD equilibrium data. For reasons as yet unknown, the attempt to autotask this routine that reads in the data caused the code to yield an incorrect eigenvalue. The computational time spent

in this routine, however, is negligible. Consequently, a successful parallelization of the interface routine is not expected to improve the performance of the code in a significant way.

The design of TERPSICHORE always envisaged an eventual attempt to parallelize the program. It was originally our intention to try to multitask the most time consuming subroutines. However, the high level of parallelism achieved with the autotasking features available on the latest generation Cray computers reduces considerably the attractiveness of a multitasking approach because any further performance improvements that could be realized would be of very limited significance if not, in fact, counterproductive.

## 5.3. Timings

### (a) Cray-2

The Helias case we have described above ( $N=48$, $N_p=72$, $N_t=32$, $N_e=50$, $N_s=32$, $N_b=160$, $P=4$, $N_{it}=11$) was run on a 2 processor Cray-2 in unitasking mode. The original version of TERPSICHORE written purely in Fortran took 228 seconds which corresponds to a rate of 130 Mflop/s.

### (b) Eight processor Cray-YMP parallelized

Performance tests of the TERPSICHORE code were also carried out on the sn1001 Cray-YMP/832 computer. This machine has 8 processors, a 32 Megaword memory and a 6.41 ns clock period. The TERPSICHORE version used in the previous subsection was run first to produce the benchmark results. Subsequently, all calculations were performed with the improved version of the code in which all double Fourier flux tube integrals are treated with successive applications of the MXM routine. For the Helias case under consideration, the number of floating point operations increased to approximately $3.49 \times 10^{10}$. The machine was dedicated to these tests. The results and performance of the code are summarized in the table below:

## Table

| | Original TERPSICHORE Unitasking | Improved TERPSICHORE Unitasking | Improved TERPSICHORE Microtasking |
|---|---|---|---|
| CPU time | 157.02" | 137.06" | 149.85" |
| Wall clock time | | 137.21" | 20.44" |
| Parallelization | 1 | 1 | 7.35 |
| Gflop/s | 0.189 | 0.255 | 1.708 |
| Operations | $29.6 \times 10^9$ | $34.9 \times 10^9$ | $34.9 \times 10^9$ |

Of the figures shown in the table, we would like to draw particular attention to the high level of parallelization of 7.35 in an eight processor machine achieved with the Cray Research autotasking utilities and to the 1.708 Gflop/s performance obtained.

Noting that the number of operations in the improved version of the code was increased relative to the original version, we can define an effective performance of $1.708 \times 29.6/34.9 = 1.449$ Gflop/s. On a YMP/8 machine with a cycle time of 6 ns instead of 6.41 ns, one expects 1.825 Gflop/s instead of 1.708 Gflop/s.

## Acknowledgments

# References :

[1]    R. Gruber, F. Troyon, D. Berger, L.C. Bernard, S. Rousset, R. Schreiber, W. Kerner, W. Schneider, K.V. Roberts, ' ERATO stability code', Comput. Phys. Commun. **21**(1981)323-371
       R. Gruber, S. Semenzato, F. Troyon, T. Tsunematsu, W. Kerner, P. Merkel, W.Schneider, 'HERA and other extentions of ERATO', Comput. Phys. Commun. **24**(1981)363-376


[2]    R.C. Grimm, J.M. Greene, J.L. Johnson, ' Computation of the MHD spectrum in axisymmetric toroidal confinement systems', Meth. Comput. Phys. **16**(1976)253-280


[3]    J. Manickam, R.C. Grimm, R.L. Dewar, ' The linear stability analysis of MHD models in axisymmetric toroidal geometry', Comput. Phys. Commun. **24**(1981)355-361


[4]    L.M. Degtyarev, S.Yu. Medvedev, ' Methods for numerical simulation of ideal MHD stability of axisymmetric plasmas ', Comput. Phys. Commun. **43**(1986)29-56


[5]    R. Gruber, J. Rappaz, ' Finite element methods in linear ideal MHD', *Springer Series in Computational Physics* (Springer Verlag,Heidelberg,1985) ISBN 3-540-13398-4


[6]    F. Troyon, R. Gruber, H. Saurenmann, S. Semenzato, S. Succi, ' MHD limits to plasma confinement', Plasma Phys. **26**(1984)209-215
       F. Troyon, R. Gruber, ' A scaling law for the beta-limit in Tokamaks', Phys. Letters **110A**(1985)29-34


[7]    D.V. Anderson, W.A. Cooper, U. Schwenn, R. Gruber, ' Linear MHD stability analysis of toroidal 3-D equilibria with TERPSICHORE', in *Proc. of the Joint Varenna-Lausanne International Workshop on theory of fusion plasmas*, (Editrice Compositori, Bologna, 1988)93-102


[8]    D.V. Anderson, A.R. Fry, R. Gruber, A. Roy, ' Gigaflop speed algorithm for the direct solution of large block-tridiagonal systems in 3-D physics applications', Computers in Physics **3**(1989)33-41

[9]     S.P. Hirshman, W.I. van Rij, P. Merkel, ' Three-dimensional free boundary calculations using a spectral Green's function method', Comput. Phys. Commun. **43**(1986)143

        S.P. Hirshman, U. Schwenn, J. Nührenberg, ' Improved radial differencing for 3D MHD equilibrium calculations',to be published in J. Comput. Phys. (1989)

[10]    J. Nührenberg, R. Zille, ' Equilibrium and stability of low-shear stellarators', in *Proc. of Workshop on theory of fusion plasmas* (Editrice Compositori, Bologna, 1987), EUR11336EN, 3-23

[11]    J. Nührenberg, R. Zille, ' Stable stellarators with medium $\beta$ and aspect ratio', Phys. Letters **114A**(1986)129-132
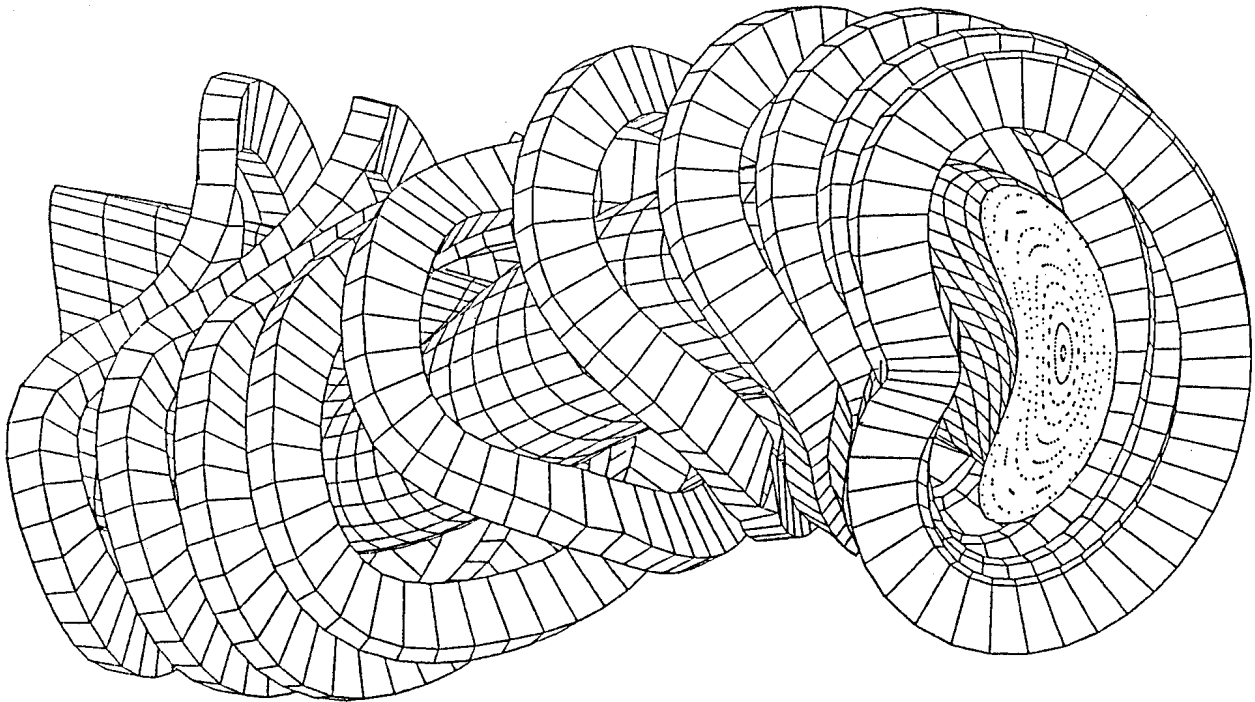
Fig. 1. The magnetic field coil structure and the plasma shape in one field period of a 4 field period Helias stellarator configuration. The cross sectional cut shows the shape of the internal flux surfaces in the plasma obtained by puncture plots left by the intersection of magnetic field lines traced over many toroidal transits across the plane defined by the cut.
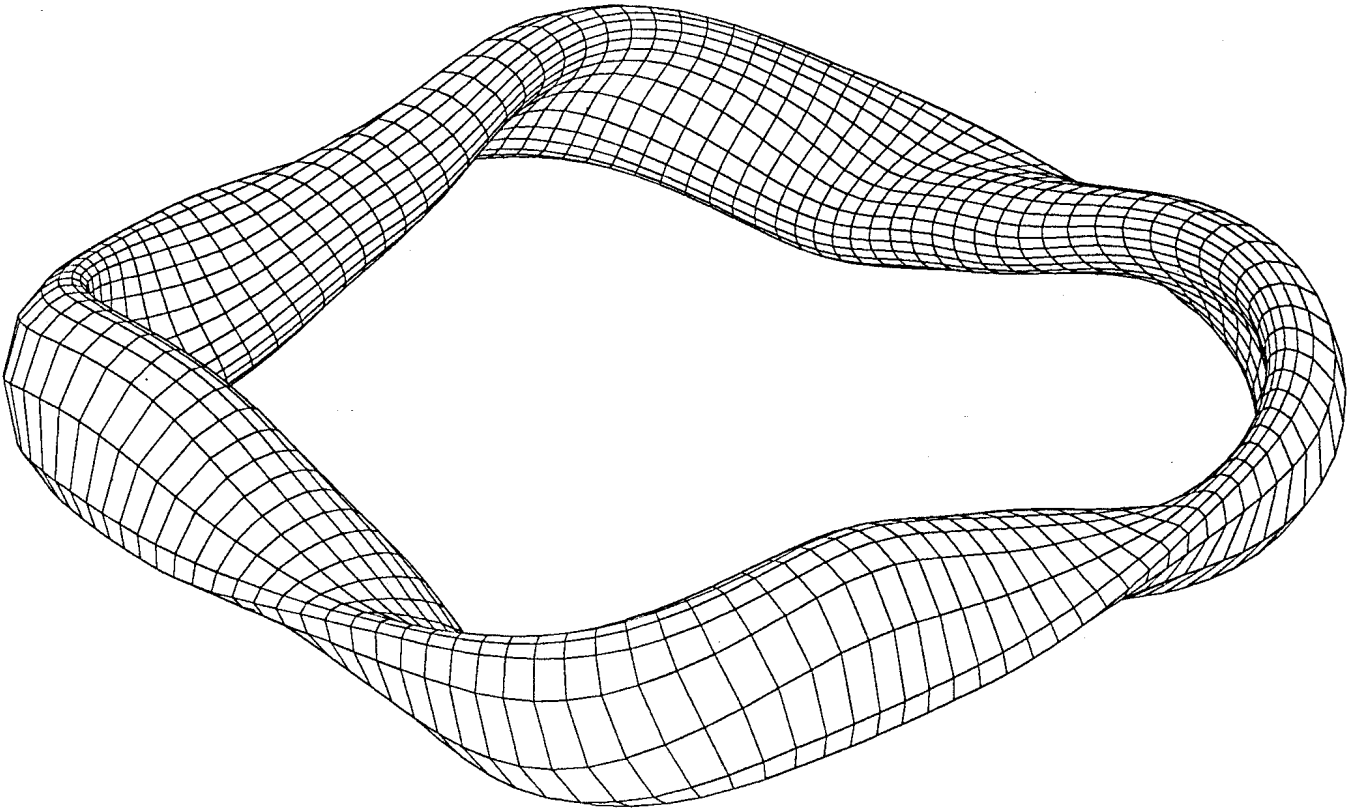
Fig. 2. The full 3D structure of a flux surface corresponding to a 4 field period Helias stellarator configuration.
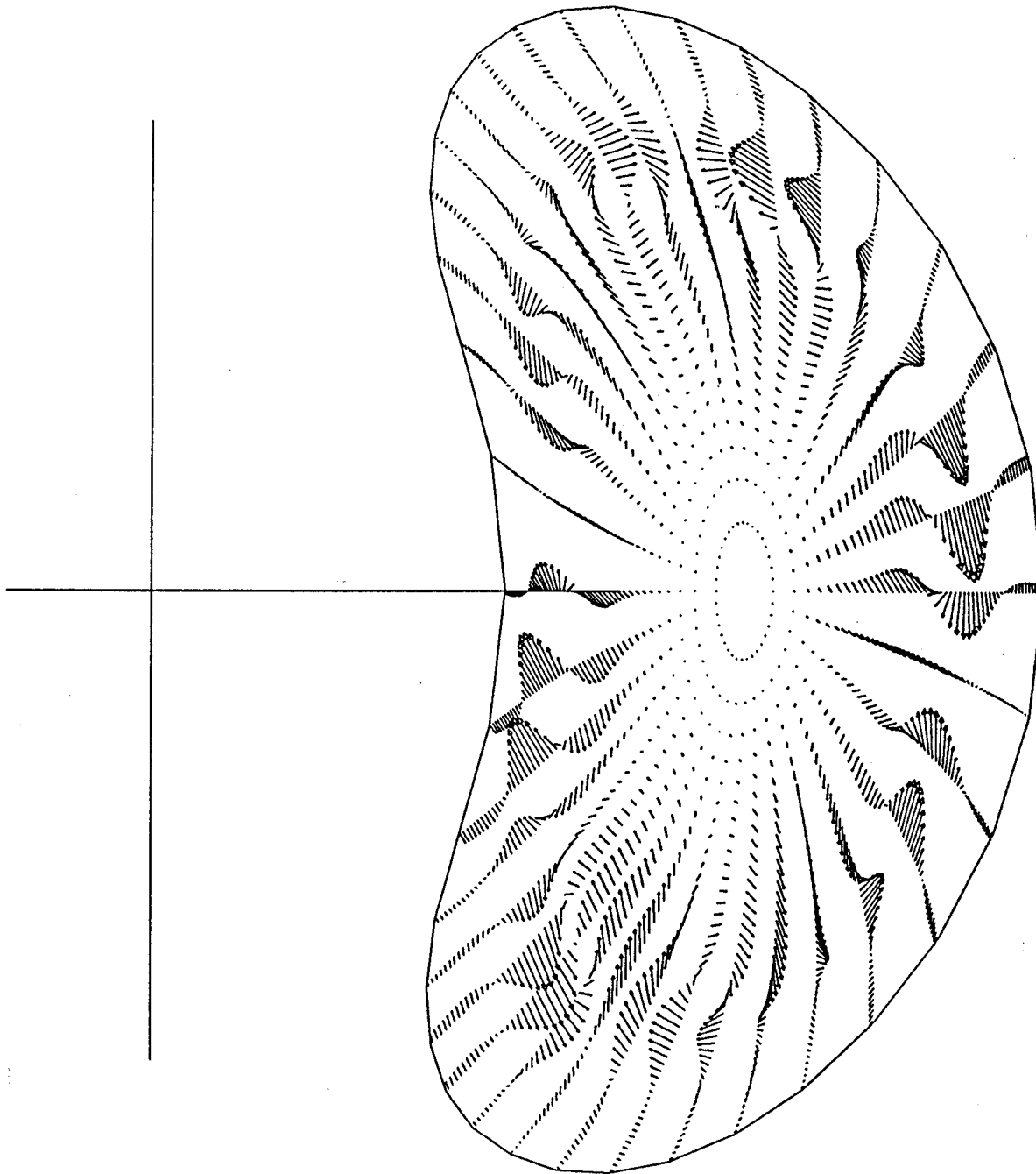
Fig. 3. The flow pattern corresponding to the most unstable eigenmode structure at the toroidal plane with Boozer coordinate toroidal angle $\phi = 0$ in a 4 field period Helias stellarator configuration. The structure is dominated by an $m = 4$, $n = 3$ mode concentrated about the $\iota = 0.75$ surface. The configuration has a plasma $\beta = 2\%$ and zero net toroidal plasma current within each flux surface.